Contents

Chapter 1

Constitutive Modelling and Parameter Determination

1.1 Introduction

A general description of the two constitutive models applied in the thesis "Application of Hypoplastic and Viscohypoplastic Constitutive Models for Geotechnical Problems" is given here. The main attention is on the procedure for the determination of the material parameters from laboratory tests and on post test numerical simulations.

1.2 Hypoplastic Constitutive Equation

The mechanical behaviour of cohesionless soil is modelled by a hypoplastic constitutive equation. It describes the changes in stress of a simple grain skeleton due to rearrangement of the grains. A simple grain skeleton is characterized by the following conditions [3]:

1. The state is defined only by the grain stress tensor $\boldsymbol{\sigma}$ and density (void ratio e).
2. The grains are permanent, i.e. there is no abrasion and grain fracturing.
3. There is an upper (e_i) and a lower limit (e_d) of the void ratio – macropores are not allowed for – depending on the effective mean pressure $p' = -\mathrm{tr}\boldsymbol{\sigma}'/3$. The same holds for the critical void ratio e_c, which is reached after large monotonic shearing.
4. Independently from the initial state proportional deformation paths lead asymptotically to proportional stress paths.

5. The mechanical behaviour of the grain skeleton is rate-independent and the principle of effective stress holds.

6. Cementation and attractive/repulsive forces of the grain contacts are negligible.

A general form of a constitutive equation for a simple grain skeleton is

$$\dot{\boldsymbol{\sigma}} = \mathbf{f}(\boldsymbol{\sigma}, \dot{\boldsymbol{\varepsilon}}, e) \tag{1.1}$$

Thereafter, the stress rate $\dot{\boldsymbol{\sigma}}$ is a function of the stress state $\boldsymbol{\sigma}$ itself, density (void ratio e) and the strain rate $\dot{\boldsymbol{\varepsilon}}$. The function $\mathbf{f}$ is 1^{st} order homogenous with respect to the strain rate ($\mathbf{f}(\lambda\dot{\boldsymbol{\varepsilon}}) = \lambda\mathbf{f}(\dot{\boldsymbol{\varepsilon}})$, i.e. rate independence) and directionally homogenous w.r.t. stress ($\vec{\mathbf{f}}(\lambda\boldsymbol{\sigma}) = \lambda\vec{\mathbf{f}}(\boldsymbol{\sigma})$). Note that the strain tensor $\boldsymbol{\varepsilon}$ does not appear in (1.1). In this work, the version of the hypoplastic constitutive equation by von Wolffersdorff (1.1) is applied. For detailed descriptions of the model please refer to e.g. [10], [4], [5] or [7].

One advantage of this model is the rather simple determination of the material parameters (see next subsection) by means of standard laboratory tests, i.e. shear (triaxial, simple or direct shear) and oedometric tests. With one set of parameters the mechanical behaviour of a cohesionless granular material can be described realistically over a wide range of soil states relevant for geotechnical engineering purposes.

1.2.1 Procedure for the Determination of the Material Parameters

1. Limit Void Ratios $\mathbf{e_{d0}}$, $\mathbf{e_{c0}}$ and $\mathbf{e_{i0}}$

$e_{d0} \approx e_{min}$ is a lower bound void ratio of a grain skeleton at zero pressure, $e_{c0} \approx e_{max}$ is the void ratio in a critical state at zero pressure. Both, e_{min} and e_{max} are determined through standard index tests (e.g. according to ASTM D4254 and D4253). e_{i0} is an upper bound void ratio of a simple grain skeleton at vanishing pressure (without macropores). $e_{i0} \approx 1.15 \cdot e_{co}$ and $e_{d0} \approx 0.6 e_{c0}$ are simple estimates [3] which have been used successfully for more than a decade.

2. Critical Friction Angle $\boldsymbol{\varphi_c}$

The critical friction angle φ_c determines the resistance of a granulate subjected to monotonic shearing in critical state, i.e. when $\dot{\boldsymbol{\sigma}} = \mathbf{0}$ and the volumetric strain rate $\dot{\varepsilon}_v = \mathrm{tr}(\dot{\boldsymbol{\varepsilon}}) = 0$ hold. Appropriate for the determination of φ_c are drained or undrained triaxial tests, simple shear or direct shear tests on initially very loose specimens ($e \approx e_{max}$).

The simplest, fastest (and therewith cheapest) and yet reliable estimate is the angle of repose (Fig. 1.1). A hopper is lifted slowly without loosing contact with the forming cone of dried

granular material. On the surface of the cone the granulate is subjected to large monotonic shearing, therewith it may be assumed to be in a critical state. The inclination of the cone, and hence the critical friction angle, can be determined by measuring the height and diameter of the cone ($\tan\varphi_c = 2h/d$) or with a set of stencils (increments of 0.5° are sufficient).

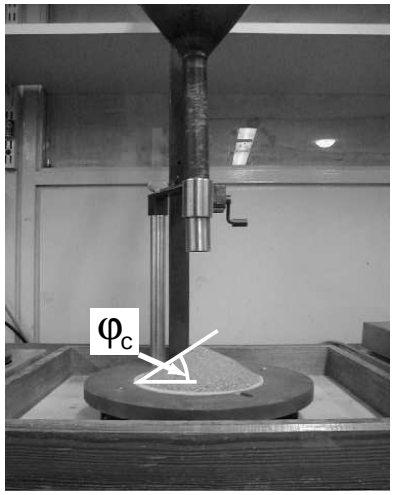

Figure 1.1: Angle of repose test.

3. Granulate Hardness h_s and Exponent n

a) In the case of an isotropic compression of a very loose sample ($e_0 = e_{max}$) the hypoplastic constitutive equation reduces to the compression law by Bauer [1]:

$$e = e_0 \cdot \exp\left[-\left(\frac{3 \cdot p'}{h_s}\right)^n\right] \tag{1.2}$$

where a referential pressure, the so-called granulate hardness h_s, together with the exponent n govern the compression for an increasing effective mean pressure p'.

For simplicity h_s and n are determined from conventional oedometric compression tests (OCT). However, it is very laborious to install a sample with $e_0 \approx e_{max}$ by moist placement [9]. Thus, h_s and n obtained by curve fitting (least square method) using (1.2) are only a first approximation.

b) The next step is to simulate the OCT with the aid of an element test programme (ETP) comprising hypoplasticity (e.g. PLAXIS (R), SoilTest) and to adjust h_s and n to match the test results.

Note: This pair of material constants also influences the curve progressions of triaxial compression test (TXC) simulation results.

4. Exponent α

The exponent α controls the peak friction angle of the material, and hence also the dilatancy behaviour. Using the results of a drained triaxial test on an initially dense sample, α can be calibrated with the aid of the ETP. But as mentioned above, h_s and n also influence the calculation results of the triaxial test simulation, thus it might be necessary to adjust these values, too.

5. Exponent β

The stiffness of a grain skeleton with $e < e_c$ can be adjusted via the exponent β. It can be calibrated with the aid of ETP simulations of an OCT on an initially dense specimen and the subsequent comparison with actual test results. It also influences the initial stiffness during TXC. As a first estimate or when lacking experimental data $\beta \approx 1.0$ has often proved satisfactory.

Calibration steps 3b to 5 are interrelated, therefore the final set of parameters has to be found iteratively. The "abort criterion" is the engineering judgement of the user and in general depends on the desired application. E.g. special attention may be paid to the correct reproduction of compressibility of dense specimen at very high pressures ($p' \geq 10\,\mathrm{MPa}$) as in the case of the interpretation of CPTs in cohesionless soils.

Example

Results of an OCT on a loose and a dense sample and one drained TXC on a dense sample of Dubai sand are used for the demonstration of the procedure developed for the determination of the hypoplastic material parameters. Furthermore, the limit void ratios, the grain size distribution, the grain density and the angle of repose were determined.

1. Parameters obtained directly from index tests:

$$\begin{aligned} e_{d0} &\approx e_{\min} = 0.762 \\ e_{c0} &\approx e_{\max} = 1.223 \\ e_{i0} &\approx 1.15 e_{\max} = 1.406 \end{aligned}$$

2. Angle of repose: $\varphi_c = 37.7°$

3. (a) h_s and n from curve fitting using (1.2) and the results of an OCT with $e_0 = 1.085$ or $I_{D0} = 27\%$, respectively (Fig. 1.2a).

   (b) h_s and n are slightly adjusted to better fit the ETP calculation results with $\alpha = 0.1$ and $\beta = 1.0$ (Fig. 1.2b, the numbers #x specify sets of parameters which are listed in Table 1.1 to demonstrate the calibration process and to show the effect of the changes in the parameters on the calculation results.)

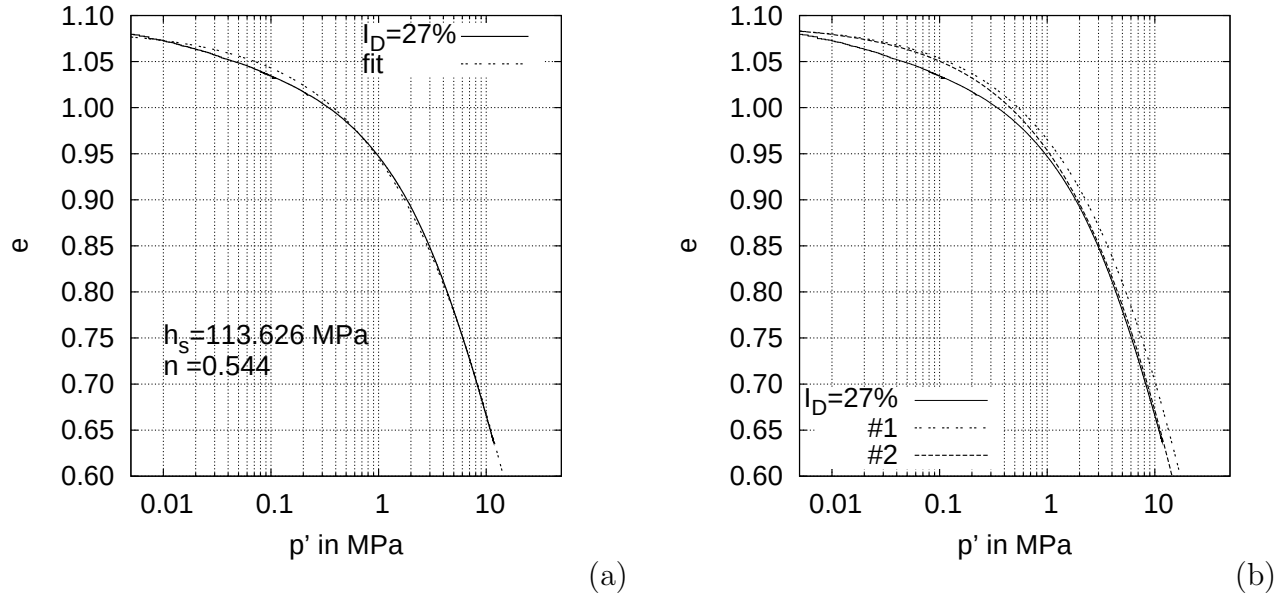

Figure 1.2: Calibration of h_s and n using OCT data: (a) first approximation (b) calibration with ETP.

4. After the simulation of the drained triaxial test n was slightly reduced to fit the curve progression in Fig. 1.3a (#3) with respect to the axial strain ε_1 at the peak $\max q$, then α is increased for a better approach of $\max q$ (#4).

5. Simulation of the OCTs on initially loose and dense samples, respectively, and calibration of β (Fig. 1.4): Parameter set #4 resulting from step 4 is used for the simulation of the two OCTs, and β is slightly increased in order to better reproduce the stiffness of the dense specimen for $p' > 10\,\mathrm{MPa}$. With the new set #5 the test on the loose specimen is recalculated, and a satisfying result is obtained. The same holds for the TXC calculated with #5 (Fig. 1.5). Otherwise steps 3b to 5 would have been repeated until a satisfactory curve fit is achieved.

In Appendix A a more comprehensive parametric study is presented to provide for a better understanding of the impact of the parameters on the mechanical response as calculated by the hypoplastic model.

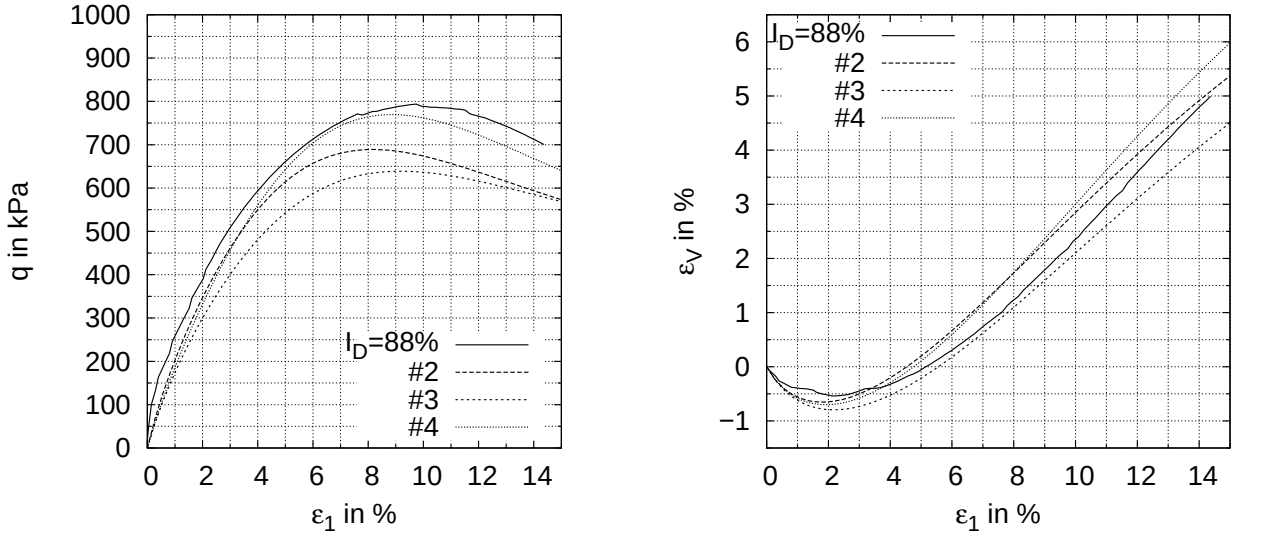

(a) (b)

Figure 1.3: Calibration of h_s, n and α using TXC data: (a) q vs. ε_1 (b) ε_v vs. ε_1.

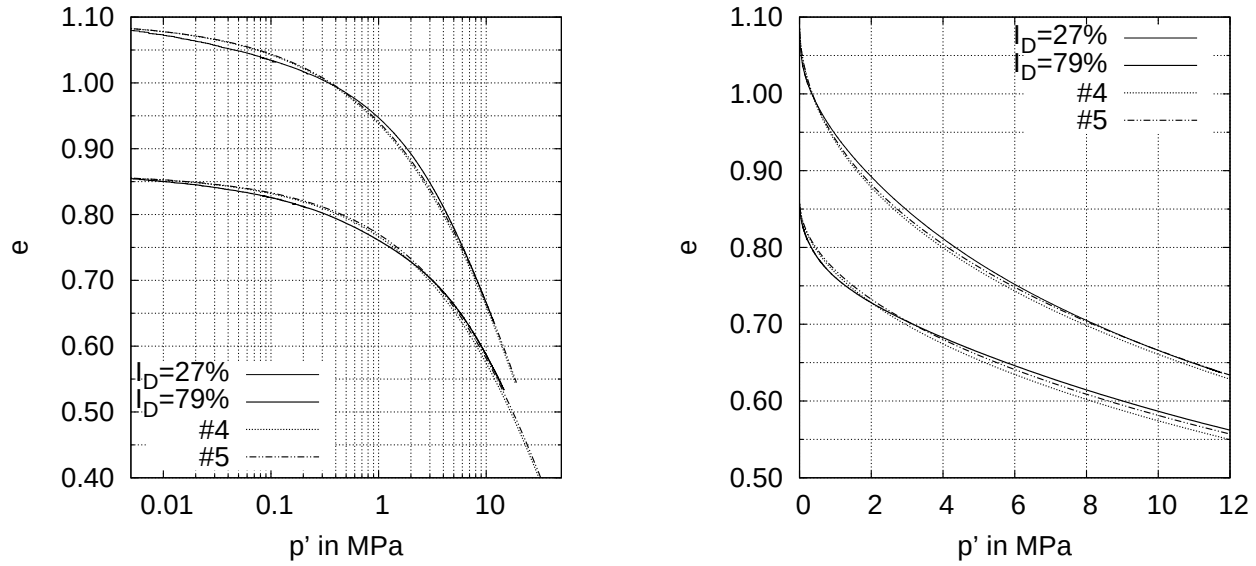

Figure 1.4: Calibration of β using OCT data.

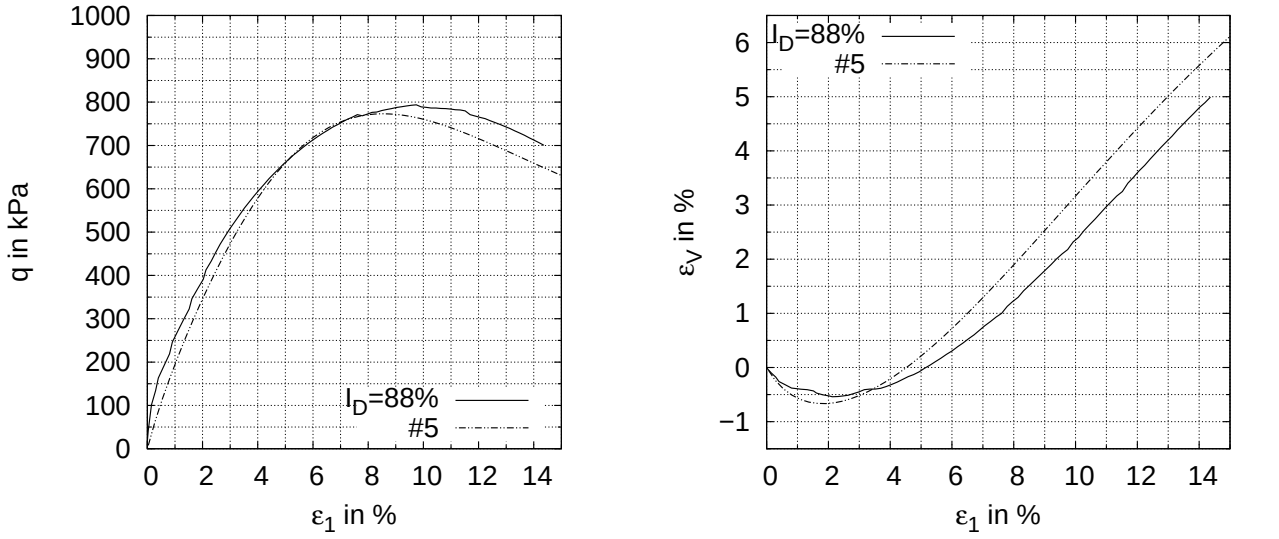

(a) (b)

Figure 1.5: Check of h_s, n and α using TXC data: (a) q vs. ε_1 (b) ε_v vs. ε_1.

#	h_s in MPa	n	α	β	Test result used
0	113.6	0.544	—	—	OCT (loose)
1	113.6	0.544	0.10	1.0	OCT (loose)
2	**95.0**	0.544	0.10	1.0	OCT (loose)
3	95.0	**0.500**	0.10	1.0	TXC (dense)
4	95.0	0.500	**0.13**	1.0	TXC (dense)
5	95.0	0.500	0.13	**1.1**	OCT (dense)

Table 1.1: Sets of parameters during the calibration process (OCT – oedom. comp., TXC – triaxial comp.).

1.3 Intergranular Strain

Both constitutive models were used with the so-called intergranular strain extension. The intergranular strain tensor $\boldsymbol{\delta}$ stores the most recent deformation history and provides for an increase in a kind of incremental stiffness $E = d\mathbf{T}/d\boldsymbol{\varepsilon}$ in the case of a change in the direction of deformation $(\mathbf{D})^{\rightarrow}$.

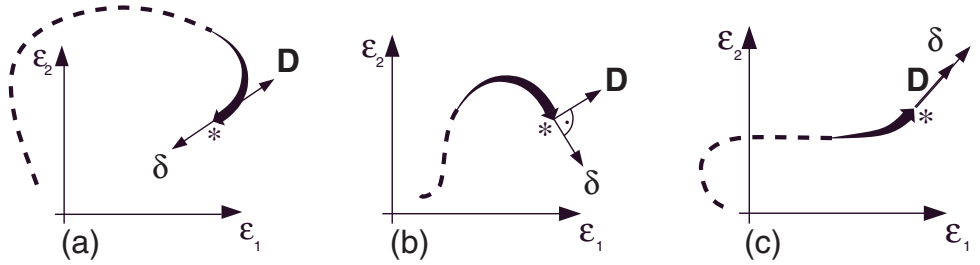

Figure 1.6: Direction of $\boldsymbol{\delta}$ and $\mathbf{D}$ after a change in direction of (a) 180°, (b) 90° and (c) after large monotonic deformation [7].

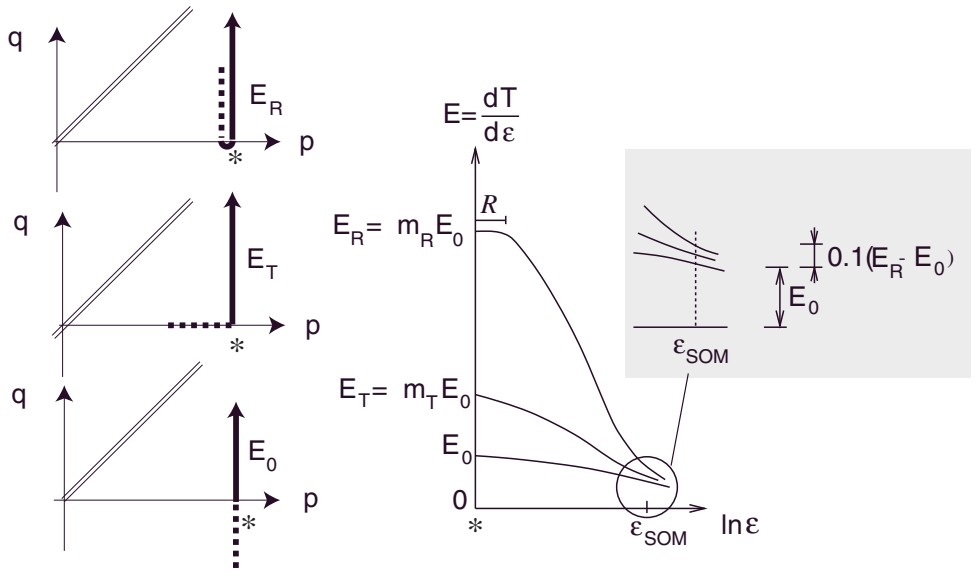

Figure 1.7: Increase of incremental stiffness due to change in the direction of deformation [7].

Suppose that density and stress are the same at point * despite different deformation paths. A 180° reversal (Fig. 1.6a) leads to $E_R = m_R \cdot E_0$ (Fig. 1.7), where the factor m_R is assumed to be a material constant and E_0 is the stiffness after long monotonic shearing and the same state. A change in direction of 90° (Fig. 1.6b) leads to $E_T = m_T \cdot E_0$. With ongoing proportional shearing after a change in direction the intergranular strain tensor $\boldsymbol{\delta}$ gradually takes the direction of $\mathbf{D}$. When the angle between $\mathbf{D}$ and δ vanishes, i.e. for $\vec{\mathbf{D}} : \vec{\delta} = \mathbf{1}$, after a sufficient proportional deformation ϵ_{SOM} the effect of the change in direction is swept out of memory [2].

Altogether there are five additional material parameters. Apart from m_R and m_T there is the quantity R which is related to (but not identical with) the elastic strain range, and there are two exponents β_χ and χ which are used to adjust the decay of $E_{R/T}$ during proportional shearing after a change in direction.

Without this extension both models produce excessive ratcheting in the case of cyclic loading, as shown in Figure 1.8b for oedometric compression and (d) for triaxial shearing. The intergranular strain extension removes this shortcoming (a and c).

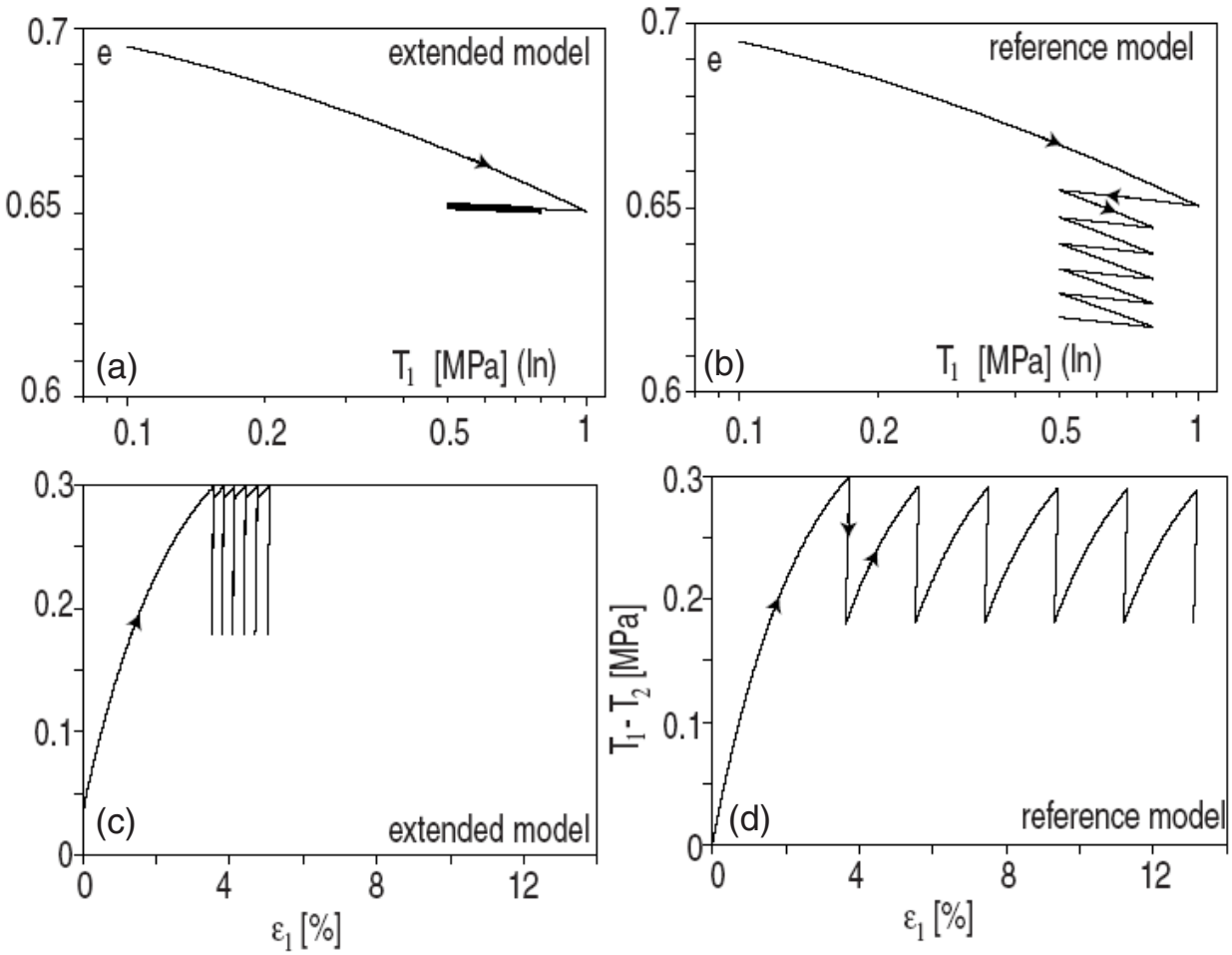

Figure 1.8: Comparison between reference model without and the extended model with intergranular strain: (a),(b) oedometric compression (c),(d) triaxial shearing [7].

1.3.1 Determination of the Parameters

Alongside with the intergranular strain model Niemunis and Herle [8] proposed a method for the determination of the additional parameters which is based on theoretical considerations.

The set of parameters they gave for one sand was used successfully for many FE simulations of boundary value problems without further experimental investigations.

However, the evaluation of dynamic (resonant column) and cyclic tests (oedometric compression and triaxial shearing) revealed that the parameter m_R should depend on the stress state and density. Figure 1.9 depicts the results of RC tests on Karlsruhe sand together with post test calculation results. If calibrated to match the $G/G_{max}^{measured}$ vs. $\ln\gamma$ curve for $p_0' = 320\,\text{kPa}$ an $m_R = 6$ is obtained (a) and for $p_0' = 20\,\text{kPa}$ an $m_R = 12$ (b).

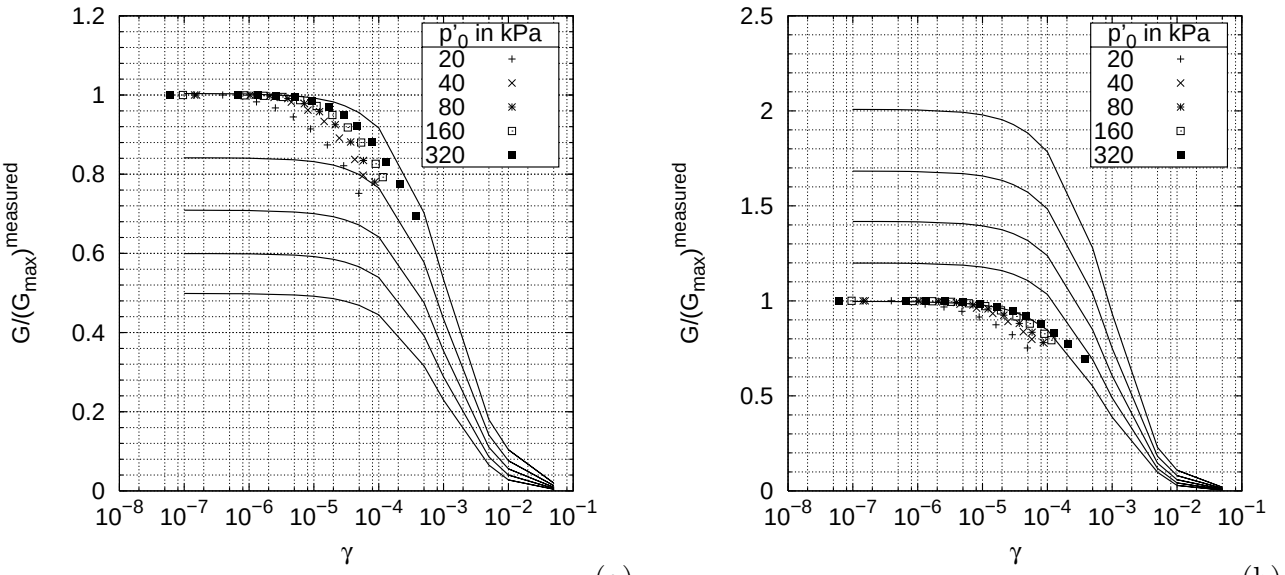

Figure 1.9: Results of RC tests performed by S. Richter on Karlsruhe sand ($e = 0.52 = \text{const.}$ compared with post test calculations with (a) $m_R = 6$ and (b) $m_R = 12$.

Cyclic oedometric compression tests on Zbraslav sand showed that m_R should also depend on density. For the same (vertical) stress $\sigma_v = -185\,\text{kPa}$ an $m_R \approx 4.3$ was obtained from tests on initially loose samples ($e_0 = 0.90$) and $m_R \approx 3.0$ in the case of $e_0 = 0.62$ [6]. Thus, a mean value should be taken, to best fit the experimental results in a relevant range of stresses and densities.

It is conjectured that the stress and density dependence also holds for m_T, but there has not been a comprehensive experimental study with regard to the determination of the intergranular strain parameters. The parameters used in this study are given in Table 1.2. Experience has shown that $R = 10^{-4}$ can be treated as a material independent constant, and that $\chi = 1.0$ together with $\beta_\chi = 0.1$ are good starting values for calibration. Using the results of e.g. oedometric compression tests with at least one unloading/reloading cycle m_R and β_χ can be calibrated in order to represent realistically, the increase in stiffness after a deformation reversal, and the range of influence ϵ_{SOM} (in the sense of Fig. 1.7).

	R	m_R	m_T	χ	β_χ
sands	10^{-4}	5	2	1.0	0.10 – 0.60
clays	10^{-4}	7	7	1.0	0.03 – 0.10

Table 1.2: Intergranular strain parameters.

In the framework of this thesis m_R and m_T were taken as proposed in [8] for sands. For clays $m_R(= m_T)$ was calibrated as depicted in Figure 1.10a to best fit the laboratory test results. For both groups of soils β_χ was calibrated so that the shape of the hysteresis loop ís reproduced realistically. Reducing β_χ leads to an increase of ϵ_{SOM}.

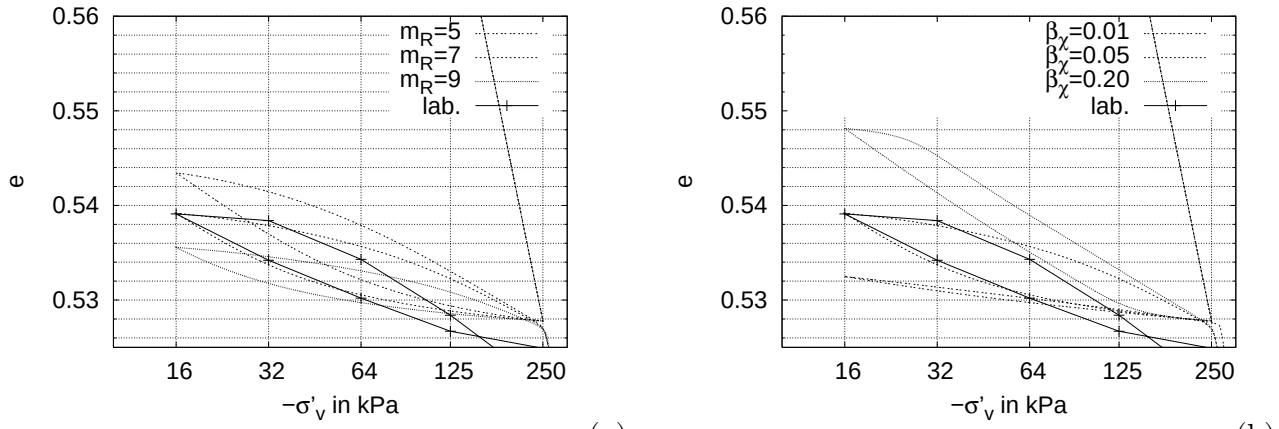

(a) (b)

Figure 1.10: Oedometric compression test result (material #160) and post test calculations (a) $\beta_\chi = \text{const.} = 0.05$ (b) $m_R = \text{const.} = 7.0$.

Bibliography

[1] E. Bauer. *Zum mechanischen Verhalten granularer Stoffe unter vorwiegend oedometrischer Beanspruchung*. PhD thesis, Veröffentlichungen des Instituts für Bodenmechanik und Felsmechanik / Universität Karlsruhe, 1992. Heft 130.

[2] G. Gudehus, M. Goldscheider, and H. Winter. Mechanical Properties of sand and clay and numerical integration methods: Some sources of errors and bounds of Accuracy. In Gudehus, editor, *Finite Elements of Geomechanics*, pages 121–150. John Wiley, New York, 1977.

[3] I. Herle. *Hypoplastizität und Granulometrie einfacher Korngerüste*. PhD thesis, Veröffentlichungen des Instituts für Bodenmechanik und Felsmechanik / Universität Karlsruhe, 1997. Heft 142.

[4] I. Herle. A relation between parameters of a hypoplastic constitutive model and grain properties. In Adachi, Oka, and Yashima, editors, *Conf. on Localization and Bifurcation for Soils and Rocks*. Balkema, 1998.

[5] I. Herle and G. Gudehus. Determination of parameters of a hypoplastic constitutive model from properties of grain assemblies. *Mech. Cohes.-Frict. Mater.*, 4(5):461–486, 1999.

[6] T. Meier. Settlement of granular materials during cyclic loading, 1999. Thesis at Institute of Theoretical and Applied Mechanics, Czech Academy of Sciences.

[7] A. Niemunis. *Extended hypoplastic models for soils*. Politechnika Gdanska, Monografia nr 34, 2003. (http://www.pg.gda.pl/ aniem/an-liter.html).

[8] A. Niemunis and I. Herle. Hypoplastic model for cohesionless soils with elastic strain range. *Mech. Cohes.-Fric. Mater.*, 4(2):279–299, 1997.

[9] R. Verdugo and K. Ishihara. The steady state of sandy soils. *Soils and Foundations*, 36(2):81–91, 1996.

[10] P. v. Wolffersdorff. A hypoplastic relation for granular materials with a predefined limit state surface. *Mech. Cohes.-Fric. Mater.*, 1:251–271, 1996.

Appendix A

Parameter Calibration – Parametric Study

The influence of a variation of the parameters h_s, n, α and β on the simulation results of oedometric compression tests and drained triaxial tests is shown in the following diagrams (Fig. A.1 to A.5). The conclusions of this parametric study are summarized in Table A.1.

Parameter	**Major Influence**	**Minor Influence**
$\boldsymbol{\alpha}$	*Drained Triaxial Shearing*	
	$\max(q)$ shear stiffness $dq/d\varepsilon_1$ ε_v	$\varepsilon_1^{\text{peak}} := \varepsilon_1(\max(q))$ $dq/d\varepsilon_1(\varepsilon_1 << \varepsilon_1^{\text{peak}})$
	Oedometric Compression	
	negligible	
$\boldsymbol{\beta}$	*Drained Triaxial Shearing*	
	$dq/d\varepsilon_1(\varepsilon_1 < \varepsilon_1^{\text{peak}})$ $\varepsilon_1(\max(q))$	$\max(q)$ ε_v
	Oedometric Compression	
	initial bulk modulus (dp'/dV)	
	dense samples	loose samples
$\mathbf{h_s},\ \mathbf{n}$	on everything	none

Table A.1: Summary of the parametric study.

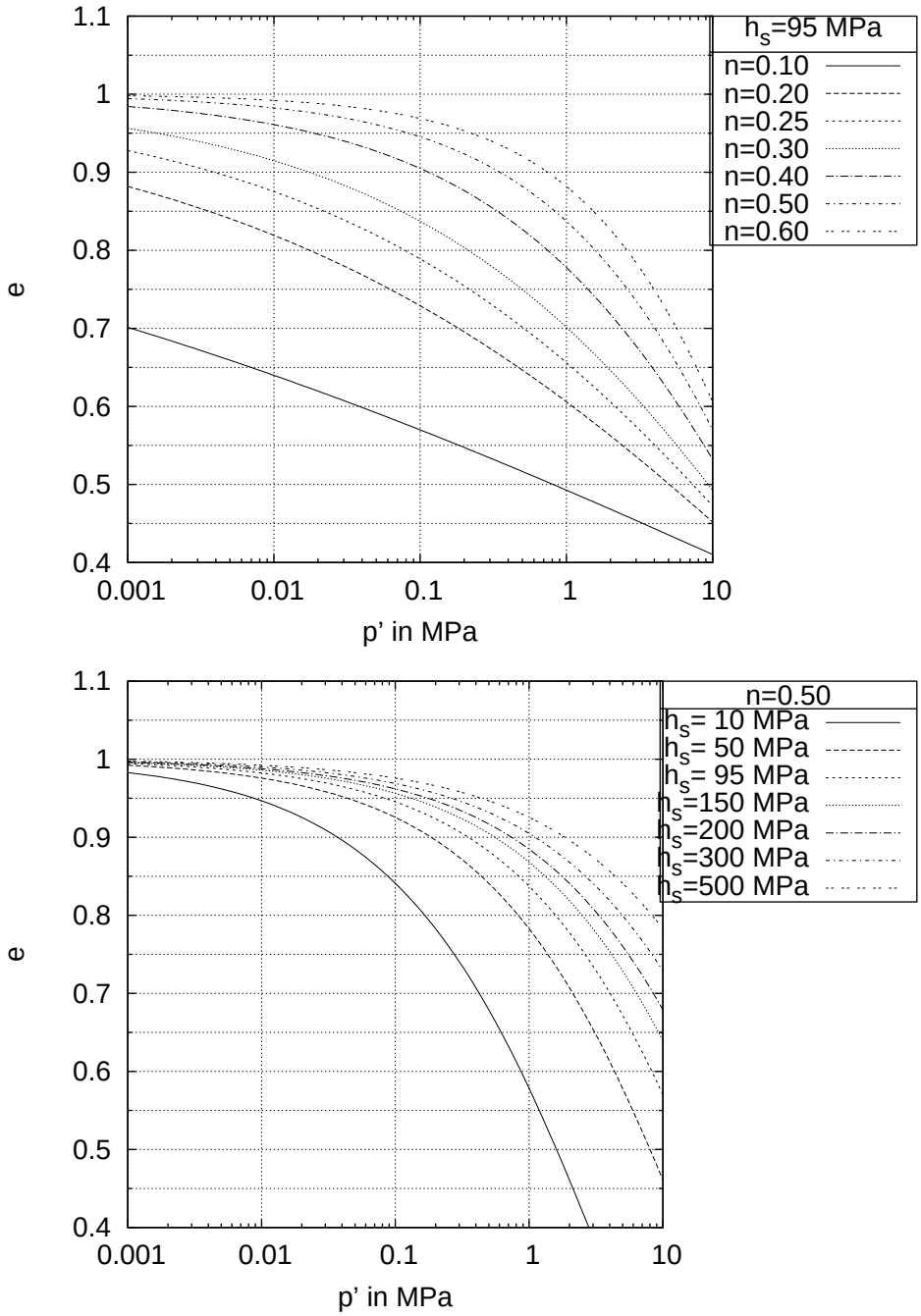

Figure A.1: . Influence of h_s and n on the oedometric compression lines calculated with Eq. (1.2).

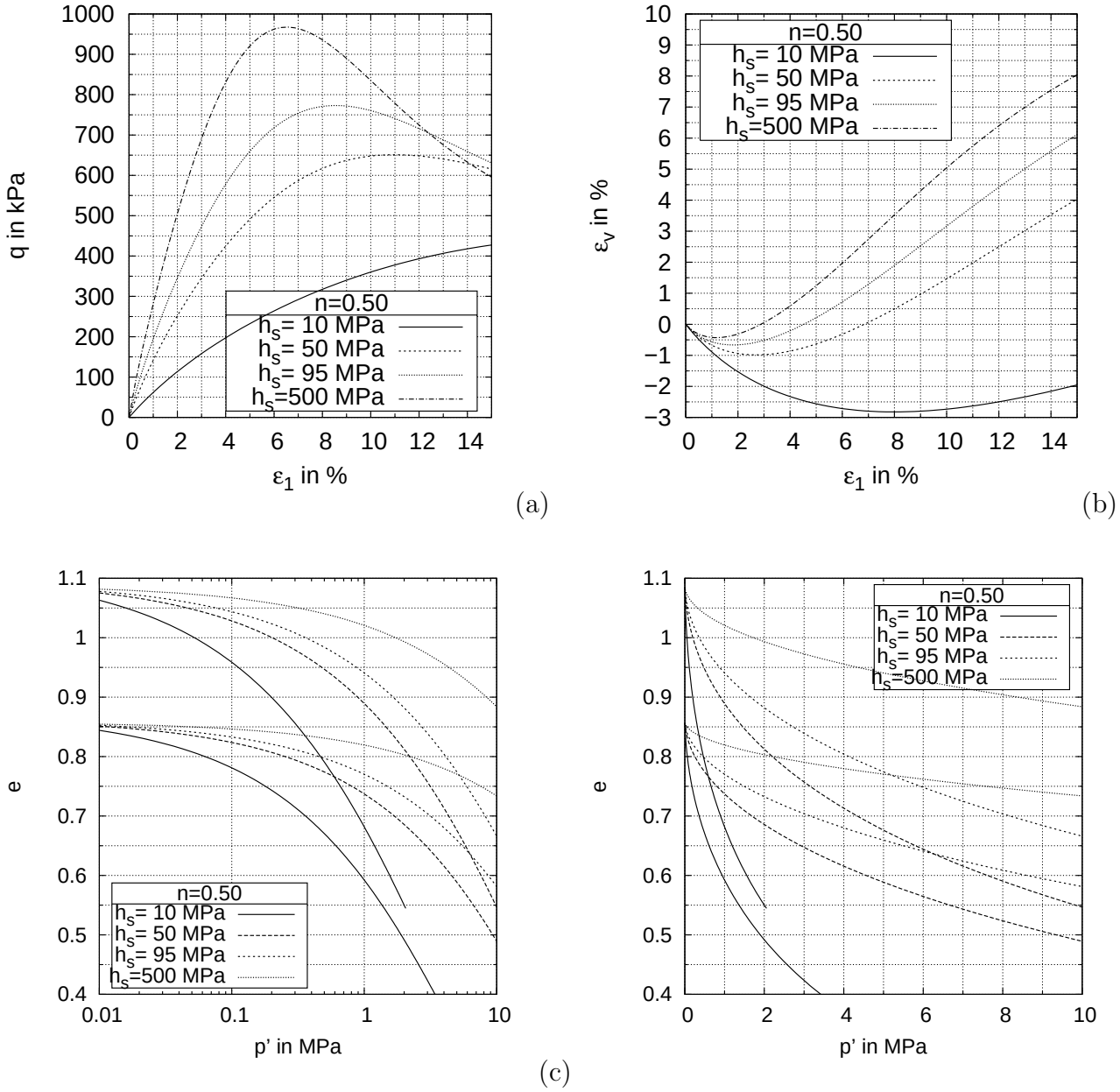

Figure A.2: Influence of a variation of h_s on (a) deviatoric stress q and (b) volumetric strain ε_v during drained triaxial shearing ($I_{D,0} = 0.88$) and (c) oedometric compression lines ($I_{D,0} = 0.27$ and $I_{D,0} = 0.79$).

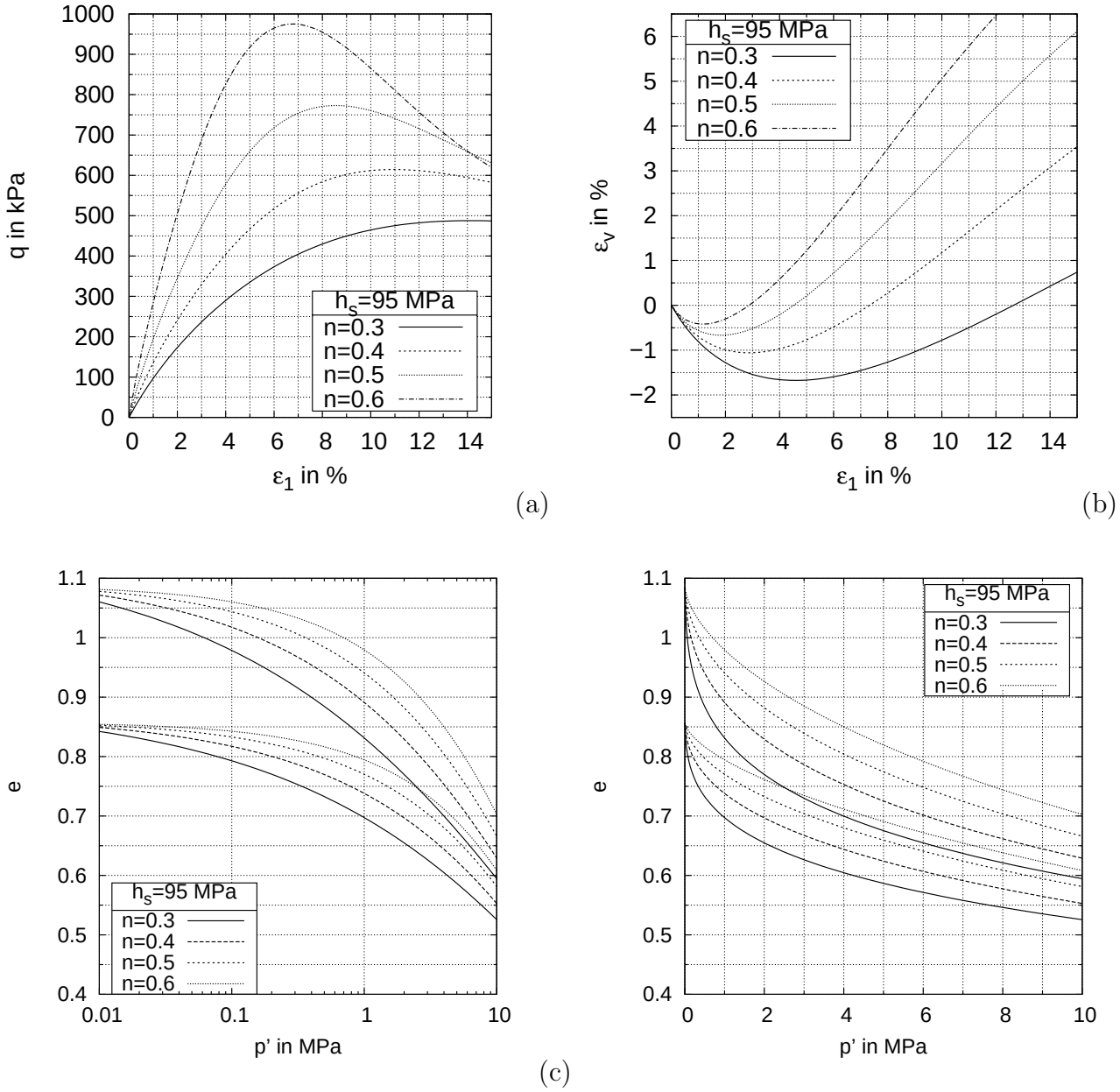

Figure A.3: Influence of a variation of n on (a) deviatoric stress q and (b) volumetric strain ε_v during drained triaxial shearing ($I_{D,0} = 0.88$) and (c) oedometric compression lines ($I_{D,0} = 0.27$ and $I_{D,0} = 0.79$).

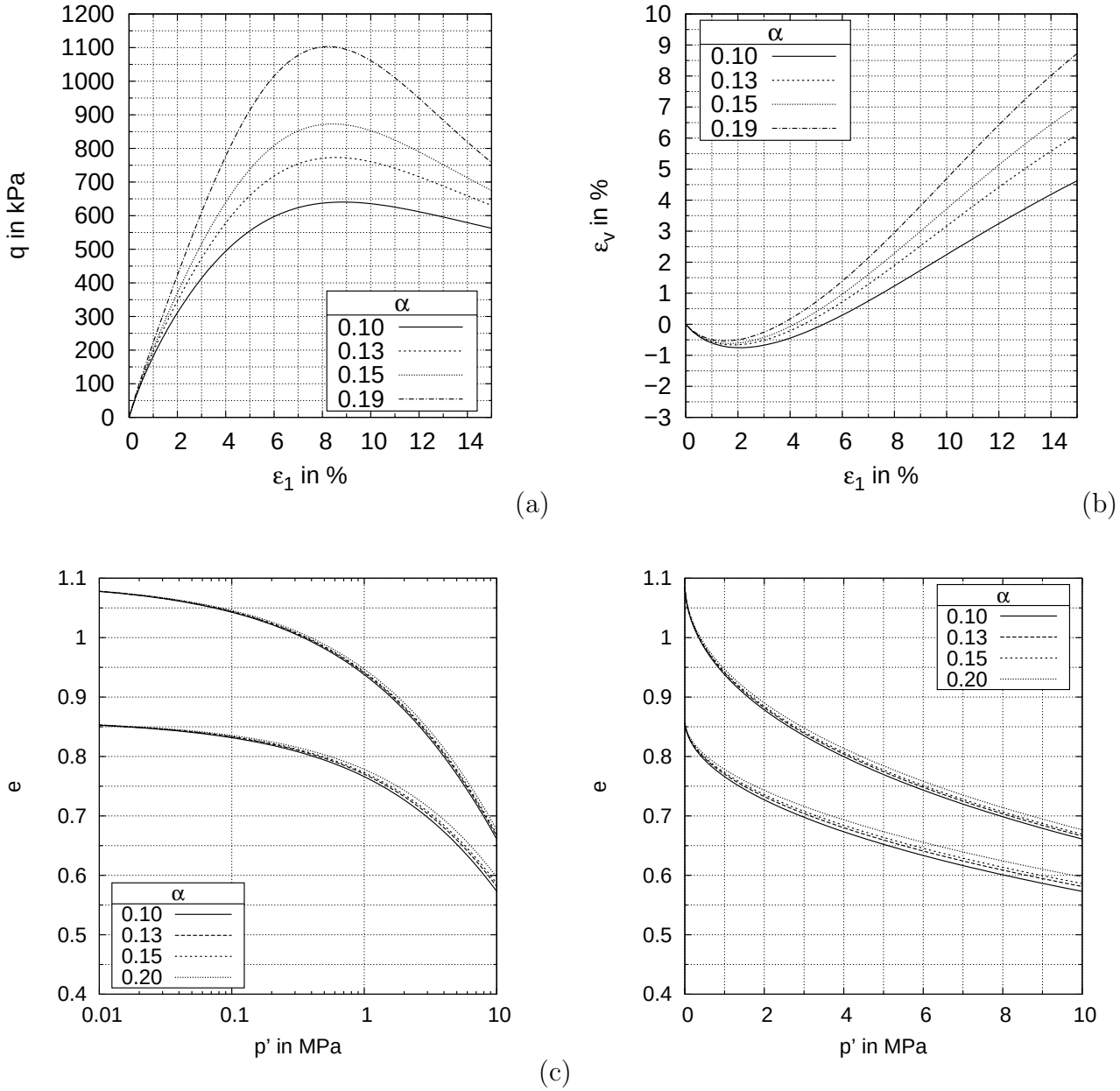

Figure A.4: Influence of a variation of α on (a) deviatoric stress q and (b) volumetric strain ε_v during drained triaxial shearing ($I_{D,0} = 0.88$) and (c) oedometric compression lines ($I_{D,0} = 0.27$ and $I_{D,0} = 0.79$).

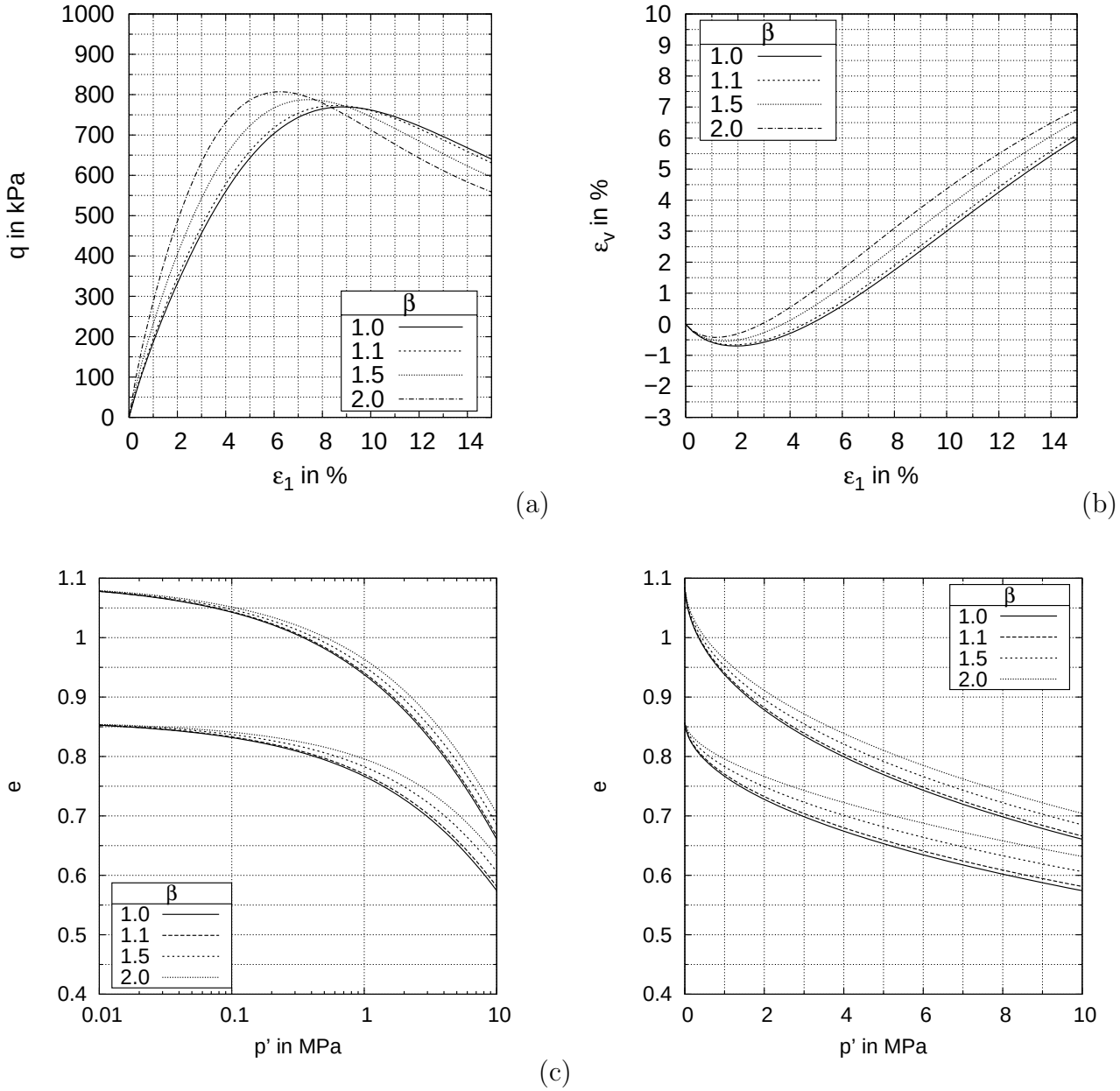

Figure A.5: Influence of a variation of β on (a) deviatoric stress q and (b) volumetric strain ε_v during drained triaxial shearing ($I_{D,0} = 0.88$) and (c) oedometric compression lines ($I_{D,0} = 0.27$ and $I_{D,0} = 0.79$).